

Ultrafast All-Optical Graphene Modulator

Wei Li,^{†,⊥} Bigeng Chen,^{†,⊥} Chao Meng,[†] Wei Fang,[†] Yao Xiao,[†] Xiyuan Li,[†] Zhifang Hu,[†] Yingxin Xu,[†] Limin Tong,^{*,†} Hongqing Wang,[‡] Weitao Liu,^{*,‡} Jiming Bao,[§] and Y. Ron Shen^{‡,||}

[†]State Key Laboratory of Modern Optical Instrumentation, Department of Optical Engineering, Zhejiang University, Hangzhou 310027, China

[‡]Department of Physics, State Key Laboratory of Surface Physics, Laboratory of Advanced Materials and Key Laboratory of Micro and Nano Photonic Structures (Ministry of Education), Fudan University, Shanghai 200433, China

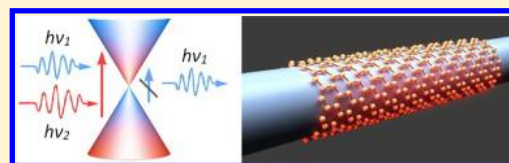
[§]Department of Electrical and Computer Engineering, University of Houston, Houston, Texas 77204, United States

^{||}Physics Department, University of California, Berkeley, California 94720, United States

Supporting Information

ABSTRACT: Graphene is an optical material of unusual characteristics because of its linearly dispersive conduction and valence bands and the strong interband transitions. It allows broadband light-matter interactions with ultrafast responses and can be readily pasted to surfaces of functional structures for photonic and optoelectronic applications. Recently, graphene-based optical modulators have been demonstrated with electrical tuning of the Fermi level of graphene. Their operation bandwidth, however, was limited to about 1 GHz by the response of the driving electrical circuit. Clearly, this can be improved by an all-optical approach. Here, we show that a graphene-clad microfiber all-optical modulator can achieve a modulation depth of 38% and a response time of ~ 2.2 ps, limited only by the intrinsic carrier relaxation time of graphene. This modulator is compatible with current high-speed fiber-optic communication networks and may open the door to meet future demand of ultrafast optical signal processing.

KEYWORDS: Graphene, microfiber, ultrafast, optical modulation



Graphene is known to exhibit a variety of exceptional electronic and photonic properties.^{1,2} Because of its unique electronic structure,^{3,4} a graphene monolayer can have a constant absorption coefficient of 2.3% over a wide spectral range from the visible to the infrared^{5,6} with the low-frequency part tunable by external fields (e.g., electrical-bias tuning of the Fermi level^{7,8} or optical excitation of carriers leading to Pauli blocking of part of the interband transitions^{9,10}). The relaxation time of the photoexcited carriers is only a few picoseconds, dominated by electron-phonon interactions and cooling of hot phonons.^{11–13} Compared to many other materials for ultrafast optics,^{14–16} graphene has the unique merit of possessing exceptionally high nonlinearity^{17,18} over a broad spectral range with ultrafast response. Being atomically thin, it is also highly flexible to be incorporated into other photonic structures.^{1,2,9,10,17,19–24} Recently, by electrically tuning the Fermi level of a graphene film,⁷ pasted onto a planar waveguide to modify the interband transitions of graphene, Liu et al. have successfully demonstrated a high-speed graphene-based optical modulator.^{21,22} The modulation bandwidth was however limited to ~ 1 GHz by the response time of the bias circuit. For future optical data processing, a modulation rate larger than 100 GHz is needed.²⁵

Obviously, the “electrical bottleneck” on the modulation rate can be circumvented by an all-optical scheme but to date graphene-based ultrafast all-optical modulation (e.g., bandwidth > 100 GHz) has not yet been reported. Here, taking the advantage of the mature platform of fiber optics, we report a

graphene-clad microfiber (GCM) all-optical modulator at ~ 1.5 μm (the C-band of optical communication) with a response time of ~ 2.2 ps (corresponding to a calculated bandwidth of ~ 200 GHz for Gaussian pulses with a time-bandwidth product of 0.44²⁶) limited only by the intrinsic graphene response time. The modulation comes from the enhanced light-graphene interaction due to optical field confined to the wave guiding microfiber^{27,28} and can reach a modulation depth of 38%.

Our GCM all-optical modulator is illustrated in Figure 1a. A thin layer of graphene is wrapped around a single-mode microfiber, which is a section with the ends tapered down from a standard telecom optical fiber. Previously, GCM structures have been reported for fiber-based mode-locking lasers^{29,30} and 1 MHz optical modulators³¹ in which the diameter of the microfiber is around 10 μm . Here, we employ subwavelength-diameter (e.g., around 1 μm diameter for C-band of optical communication) microfiber for single-mode operation.²⁸ The principle of the GCM modulator is as follows. A weak infrared signal wave coupled into the GCM experiences significant attenuation due to absorption in graphene as it propagates along. When a switch light is introduced, it excites carriers in the graphene and through Pauli blocking of interband transitions it shifts the absorption threshold of graphene to higher

Received: November 23, 2013

Revised: December 23, 2013

Published: January 7, 2014

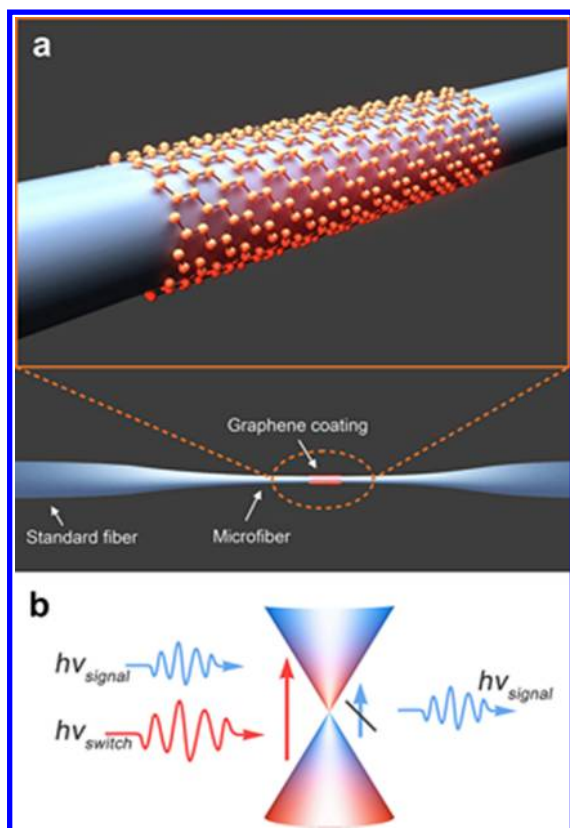


Figure 1. Schematic illustration of a GCM optical modulator. (a) A thin layer of graphene is wrapped around a microfiber that is a section tapered down from a standard telecom optical fiber. (b) Schematic describes pump and probe of carriers in the linearly dispersive valence and conduction bands of graphene. Excited carriers can lead to the band-filling effect that drastically modifies the absorption spectrum.

frequency, resulting in a much lower attenuation of the signal wave. The switch light leads to modulation of the signal output from the fiber, and its response time is limited by the relaxation of the excited carriers. The relaxation time of carrier–carrier scattering in graphene is known to be tens to hundreds of femtoseconds and that of carrier-phonon scattering ~ 1 to a few picoseconds (refs 11–13). The switch-light-induced refractive index change of the atomically thin graphene is small enough that it does not appreciably change the wave-guiding mode of the microfiber. We also note that tapering of a section of the regular fiber into a microfiber does not introduce appreciable loss [see Supporting Information Figure S1]. This allows a GCM modulator to be easily incorporated into a standard fiber-optic system for in-fiber operation.

In our experiment, we tapered down a section of a single-mode fiber (SMF 28, Corning Inc.) into a microfiber of $\sim 1 \mu\text{m}$ in diameter and $\sim 2 \text{ mm}$ in length [see Supporting Information Figure S1a]. Graphene flakes (layer numbers of 1–7 [see Supporting Information Figure S2]), prepared by micro-mechanical exfoliation³² from highly oriented pyrolytic graphite (HOPG), were transferred and wrapped around the microfiber via micromanipulation [see Supporting Information Figures S3]. Figure 2a–c shows a typical as-fabricated bilayer-graphene-clad microfiber. With a 633 nm light guided through the microfiber, the graphene-cladded area was clearly visible from the scattered light (Figure 2a,b). The scanning electron microscopy (SEM) image (Figure 2d) revealed that the graphene-cladded length was $16 \mu\text{m}$. The Raman spectrum of the graphene (Figure 2e) indicated that it was a bilayer.³³ We have also succeeded in wrapping monolayer and multilayer (>2 layers) graphene films on microfibers.

The GCM structure enables significant enhancement of light–graphene interaction via tightly confined evanescent field guided along the surface of the microfiber. Figure 3a shows

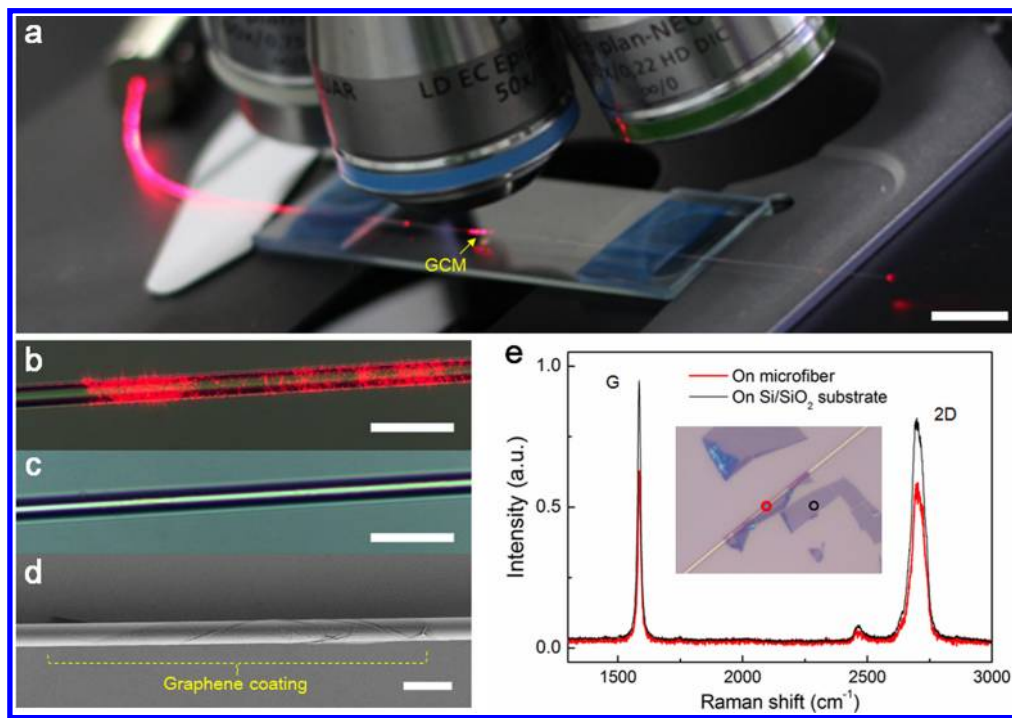


Figure 2. Sample characterization. (a) A GCM of $1.2\text{-}\mu\text{m}$ diameter guiding a 633 nm light is located under an optical microscope. The red dot beneath the objective indicates the location of the graphene cladding on the microfiber. Scale bar, 1 cm. (b,c) Optical microscope images of the GCM area with (b) and without (c) the guiding red light in the fiber. Scale bar, $5 \mu\text{m}$. (d) SEM image of the GCM. Scale bar, $2 \mu\text{m}$. (e) Raman spectra of the bilayer graphene films on the GCM and on a Si/SiO_2 wafer. Inset, optical microscope image showing the location of the bilayer graphene on GCM (red circle) and on Si/SiO_2 (black circle) for the Raman characterization.

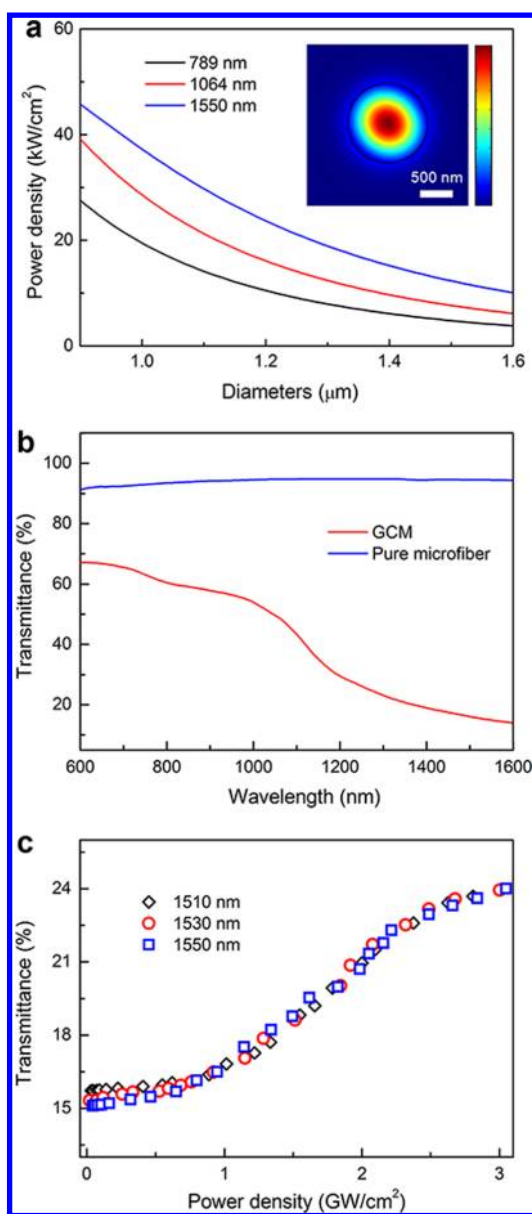


Figure 3. Optical waveguiding properties of GCM. (a) Dependence of the power density at the surface of a microfiber on the microfiber diameter for 1 mW input power (in the HE₁₁ mode) at three different wavelengths. The inset shows the cross-sectional intensity distribution in a 1.2 μm diameter microfiber for 1550 nm wavelength (calculation by COMSOL). (b) Transmission spectrum of the GCM in comparison with that of a pure microfiber. (c) Transmittance of the GCM as a function of the peak power of 220 fs pulses with 76 MHz repetition rate at several wavelengths.

calculated power density at the surface of a microfiber from a 1 mW guided wave in the HE₁₁ mode for three different wavelengths (the inset depicts the mode pattern). For reference, the power density at the surface of a 1.2 μm diameter microfiber is ~24 kW/cm² for 1550 nm wavelength.

To see how graphene cladding affects the light transmission through a microfiber we launched a continuous-wave (CW) broadband light (from a halogen lamp) through a GCM of 1.2 μm diameter with a ~20 μm cladding length. The light power was kept below 2 μW, which was not strong enough to change the absorption of graphene. Figure 3b displays the transmission spectrum of the GCM in comparison with that

of a pure microfiber. In the spectral range of 600–1600 nm, the pure microfiber has nearly constant transmittance, but the GCM has an absorption increasing with increasing wavelength, which can be explained by the higher evanescent field for longer wavelength at the graphene interface²⁸ [see also Supporting Information Figure S4]. The observed absorption of the GCM was an order of magnitude higher than that of a bilayer graphene (4.6%⁵) because of the larger effective interaction length.

At higher light intensities, the band filling (Pauli blocking) effect of the excited carriers can drastically change the absorption spectrum of graphene. To see this in our 1.2 μm GCM, we sent ~1.55 μm femtosecond pulses (76 MHz, 220 fs) through the same 1.2 μm diameter GCM and measured the dependence of transmission on the input power [see Supporting Information Figure S5]. The result is presented in Figure 3c. At a peak power density below ~0.2 GW/cm² (137 μW in average power, or 8.2 W in peak power), absorption of graphene is in the linear range, leading to a nearly constant transmittance of ~15.5%. When the density exceeds 1 GW/cm² (0.68 mW in average power, or 40.6 W in peak power), the transmittance increases rapidly due to the saturable absorption,⁹ which saturates as the density approaches ~2.5 GW/cm² (~1.7 mW in average power, or 101 W in peak power) to yield a transmittance of ~24%. As the power density we used here is kept below 3 GW/cm², the nonlinear response contributed from two-photon absorption that requires a much higher power density³⁴ is negligible.

The strong pump effect on the absorption of GCM can be readily employed for all-optical modulation. For demonstration, we showed that we could use nanosecond pump pulses to switch out signal pulses from a GCM (Figure 4a). A 1.55 μm CW signal light (from Module 2 in Figure 4a) was passed through a GCM with a fairly low transmission (by coating a 1.2 μm diameter microfiber with a 30 μm length graphene flake). When 1.06 μm ns pump laser pulses (~5 ns, 2.4 kHz, from Module 2) were also sent through the GCM with an average power of 300 μW (corresponding to a peak power of 25 W, or a peak power density of ~0.4 GW/cm²), they increased the signal transmission of the GCM during their presence and switched out the nanosecond signal pulses accordingly, which could be readily observed at the output (Figure 4b). The normalized pump-induced differential transmittance (DT) for the signal was ~30%. In this case, the observed long tail of the signal pulses (~80 ns, shown in Figure 4c) was not intrinsic but was due to the slow recovery time of the photodetector. To explore the ultrafast dynamical characteristic of the GCM, we adopted the pump–probe measurement (Figure 4a). Light from a femtosecond Ti:sapphire laser (789 nm wavelength, 35 fs duration, 1 kHz repetition rate) was split into two by a 60/40 beam splitter (BS). One after passing through a 789 nm bandpass filter (BPF) with 2 nm bandwidth (yielding a ~500 fs pulse duration) was used as the pump, and the other pumped an optical parametric amplifier (OPA) to generate 1550 nm signal (probe) pulses. They were recombined at a dichroic beam splitter (DBS1) and then coupled into a 1.4 μm-diameter GCM with a 20 μm long bilayer-graphene cladding. An adjustable delay line in the signal path before DBS1 allowed adjustable time delay between pump and probe pulses. The pump power was 200 nW (corresponding to a peak power of ~400 W or a peak power density of ~2.4 GW/cm²), while the probe power was ≤0.5 nW (≤76 MW/cm²). The measured transmission of the signal pulse as a function of the pump–probe

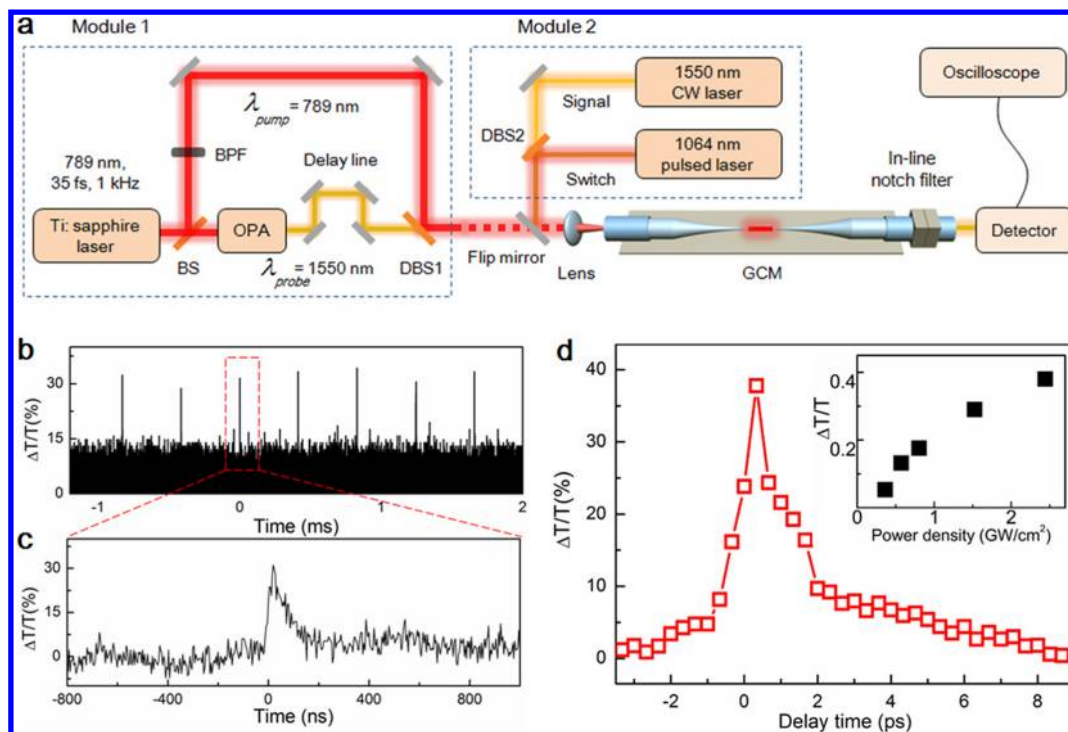


Figure 4. All-optical modulation. (a) Schematic illustration of experimental setups. Module 1: light source for pump–probe measurement. Module 2: light source for nanosecond-pulse modulation of a CW light. (b) Pulses switched out from a 1550 nm CW beam in a GCM by a 5 ns 1064 nm pump pulse train. The induced differential transmittance is $\sim 30\%$. (c) Time profile of a switched-out pulse. (d) Differential transmittance of the probe light through a $1.4\ \mu\text{m}$ GCM with $20\ \mu\text{m}$ long graphene cladding as a function of the pump–probe time delay with a pump power of 200 nW, showing a response time of ~ 2.2 ps. The inset shows the dependence of the modulation depth on pump intensity.

delay time is given in Figure 4d. The signal pulse transmission is maximum near zero pump–probe delay and has a decay time of ~ 2.2 ps (corresponding to a maximum modulation rate of ~ 200 GHz for Gaussian pulses²⁶). The signal transmittance without pump was $\sim 20\%$ and changed to $\sim 27.6\%$ with the pump at zero time delay, corresponding to a maximal modulation depth of $\sim 38\%$, which is 2 orders of magnitude higher than the modulation achievable in graphene in free-space.^{11–13} The modulation depth was found to increase monotonously with pump intensity, exhibiting only weak saturation, as seen in the inset of Figure 4d. Because the intensity for strong saturation or optical damage of graphene is much higher than the maximum pump intensity used here ($2.4\ \text{GW}/\text{cm}^2$), higher modulation depth should be achievable in GCM with further optimization.

In principle, an all-optical approach is the most promising solution to ultrafast signal processing beyond 100 GHz,²⁵ and the fiber-compatible scheme is one of the most practical strategies for future applications ranging from optical communication and sensing to ultrafast laser spectroscopy and metrology. The GCM all-optical modulation with response time of ~ 2.2 ps (corresponding to a calculated bandwidth of ~ 200 GHz for Gaussian pulses²⁶) demonstrated here, which comes from seamless integration of fiber optics and graphene photonics, may pave the way to explore the full potential of graphene-based devices for ultrafast photonics, as well as a compact approach to fiber-based ultrafast technology for future fiber-optic circuits, systems and networks.

■ ASSOCIATED CONTENT

Supporting Information

Section 1: Fabrication and characterization of optical microfibers. Section 2: Raman characterization of graphene. Section 3:

Fabrication of GCMs. Section 4: Calculated power densities of the HE_{11} mode at the surface of a microfiber. Section 5: Experimental arrangement for optical characterization of GCMs. This material is available free of charge via the Internet at <http://pubs.acs.org>.

■ AUTHOR INFORMATION

Corresponding Authors

*E-mail: (L.T.) phytong@zju.edu.cn.

*E-mail: (W.L.) wliu@fudan.edu.cn.

Author Contributions

[†]W.L. and B.C. contributed equally to this paper.

Notes

The authors declare no competing financial interests.

■ ACKNOWLEDGMENTS

We thank Y. Cao and Y. C. Wen for the help in all-optical modulation measurements and T. Y. Gu, T. Chen, B. Guo, X. S. Jiang, Z. Y. Yang, S. S. Lin, L. Y. Chen, S. L. Yu, H. T. Wang, and M. Liu for helpful discussions. This work was supported by the National Key Basic Research Program of China under Grant Agreements 2013CB328703 and 2012CB921400 and the National Natural Science Foundation of China under Grant Agreements 61036012 and 61108048. Y.R.S. was supported by the Director, Office of Science, Office of Basic Energy Sciences, Materials Sciences and Engineering Division, of the U.S. Department of Energy under Contract No. DE-AC03-76SF00098. J.M.B. acknowledges support from the National Science Foundation Career Award under Contract No. ECCS-1240510 (monitored by Anupama Kaul) and the Robert A Welch Foundation under Contract No.E-1728.

■ REFERENCES

- (1) Bonaccorso, F.; Sun, Z.; Hasan, T.; Ferrari, A. C. Graphene photonics and optoelectronics. *Nat. Photonics* **2010**, *4*, 611–622.
- (2) Avouris, P. Graphene: Electronic and Photonic Properties and Devices. *Nano Lett.* **2010**, *10*, 4285–4294.
- (3) Novoselov, K. S.; et al. Two-dimensional gas of massless Dirac fermions in graphene. *Nature* **2005**, *438*, 197–200.
- (4) Zhou, S. Y.; et al. First direct observation of Dirac fermions in graphite. *Nat. Phys.* **2006**, *2*, 595–599.
- (5) Nair, R. R.; et al. Fine structure constant defines visual transparency of graphene. *Science* **2008**, *320*, 1308.
- (6) Mak, K. F.; et al. Measurement of the optical conductivity of graphene. *Phys. Rev. Lett.* **2008**, *101*, 196405.
- (7) Wang, F.; et al. Gate-variable optical transitions in graphene. *Science* **2008**, *320*, 206–209.
- (8) Li, Z. Q.; et al. Dirac charge dynamics in graphene by infrared spectroscopy. *Nat. Phys.* **2008**, *4*, 532–535.
- (9) Bao, Q.; et al. Atomic-layer graphene as a saturable absorber for ultrafast pulsed lasers. *Adv. Funct. Mater.* **2009**, *19*, 3077–3083.
- (10) Sun, Z.; et al. Graphene Mode-Locked Ultrafast Laser. *ACS Nano* **2010**, *4*, 803–810.
- (11) Dawlaty, J. M.; Shivaraman, S.; Chandrashekar, M.; Rana, F.; Spencer, M. G. Measurement of ultrafast carrier dynamics in epitaxial graphene. *Appl. Phys. Lett.* **2008**, *92*, 042116.
- (12) Sun, D.; et al. Ultrafast relaxation of excited Dirac fermions in epitaxial graphene using optical differential transmission spectroscopy. *Phys. Rev. Lett.* **2008**, *101*, 157402.
- (13) Huang, L. B.; et al. Ultrafast Transient Absorption Microscopy Studies of Carrier Dynamics in Epitaxial Graphene. *Nano Lett.* **2010**, *10*, 1308–1313.
- (14) Almeida, V. R.; Barrios, C. A.; Panepucci, R. R.; Lipson, M. All-optical control of light on a silicon chip. *Nature* **2004**, *431*, 1081–1084.
- (15) Pacifici, D.; Lezec, H. J.; Atwater, H. A. All-optical modulation by plasmonic excitation of CdSe quantum dots. *Nat. Photonics* **2007**, *1*, 402–406.
- (16) Hu, X.; Jiang, P.; Ding, C.; Yang, H.; Gong, Q. Picosecond and low-power all-optical switching based on an organic photonic-bandgap microcavity. *Nat. Photonics* **2008**, *2*, 185–189.
- (17) Gu, T.; et al. Regenerative oscillation and four-wave mixing in graphene optoelectronics. *Nat. Photonics* **2012**, *6*, 554–559.
- (18) Hendry, E.; Hale, P. J.; Moger, J.; Savchenko, A. K. Coherent nonlinear optical response of graphene. *Phys. Rev. Lett.* **2010**, *105*, 097401.
- (19) Xia, F.; Mueller, T.; Lin, Y.-M.; Valdes-Garcia, A.; Avouris, P. Ultrafast graphene photodetector. *Nat. Nanotechnol.* **2009**, *4*, 839–843.
- (20) Mueller, T.; Xia, F.; Avouris, P. Graphene photodetectors for high-speed optical communications. *Nat. Photonics* **2010**, *4*, 297–301.
- (21) Liu, M.; et al. A graphene-based broadband optical modulator. *Nature* **2011**, *474*, 64–67.
- (22) Liu, M.; Yin, X. B.; Zhang, X. Double-Layer Graphene Optical Modulator. *Nano Lett.* **2012**, *3*, 1482–1485.
- (23) Bao, Q.; et al. Broadband graphene polarizer. *Nat. Photonics* **2011**, *5*, 411–415.
- (24) Kim, K.; Choi, J.-Y.; Kim, T.; Cho, S.-H.; Chung, H. J. A role for graphene in silicon-based semiconductor devices. *Nature* **2011**, *479*, 338–344.
- (25) Alduino, A.; Paniccia, M. Interconnects: Wiring electronics with light. *Nat. Photonics* **2007**, *1*, 153–155.
- (26) Siegman, A. E. *Lasers*; University Science Books: Mill Valley, CA, 1986.
- (27) Tong, L. M.; et al. Subwavelength-diameter silica wires for low-loss optical wave guiding. *Nature* **2003**, *426*, 816–819.
- (28) Tong, L. M.; Lou, J. Y.; Mazur, E. Single-mode guiding properties of subwavelength-diameter silica and silicon wire waveguides. *Opt. Express* **2004**, *12*, 1025–1035.
- (29) He, X. Y.; et al. Wavelength-tunable, passively mode-locked fiber laser based on graphene and chirped fiber Bragg grating. *Opt. Lett.* **2012**, *12*, 2394–2396.
- (30) Wang, J. Z.; et al. Evanescent-light deposition of graphene onto tapered fibers for passive Q-switch and mode-locker. *IEEE Photon. J.* **2012**, *4*, 1925–1305.
- (31) Liu, Z. B.; et al. Broadband all-optical modulation using a graphene-covered-microfiber. *Laser Phys. Lett.* **2013**, *10*, 065901.
- (32) Novoselov, K. S.; et al. Electric field effect in atomically thin carbon films. *Science* **2004**, *306*, 666–669.
- (33) Ferrari, A. C.; et al. Raman spectrum of graphene and graphene layers. *Phys. Rev. Lett.* **2006**, *97*, 187401.
- (34) Yang, H. Z. Giant Two-Photon Absorption in Bilayer Graphene. *Nano Lett.* **2011**, *11*, 2622–2627.